ORIGINAL PAPER

I. Abrahams · F. Krok · S. C. M. Chan · W. Wrobel ·
A. Kozanecka-Szmigiel · A. Luma · J. R. Dygas

Defect structure and ionic conductivity in $Bi_3Nb_{0.8}W_{0.2}O_{7.1}$

Abstract Defect structure and conductivity behavior are discussed in the oxide ion conductor $Bi_3Nb_{0.8}W_{0.2}O_{7.1}$. Investigations were carried out using a combination of AC impedance spectroscopy and powder X-ray and neutron diffraction. $Bi_3Nb_{0.8}W_{0.2}O_{7.1}$ shows a defect fluorite type structure with evidence for superlattice ordering in the oxide ion sublattice. A detailed analysis of the diffraction results allow for proposed models for the defect structure and suggest vacancy trapping in the six coordinate environment of Nb^{5+}/W^{6+} cations. The influence of the defect structure on ionic conductivity is discussed.

Keywords Bismuth oxide · Fluorite · Defect structure · Neutron diffraction · Impedance spectroscopy

Introduction

Fast oxide ion conduction in the high temperature δ-polymorph of Bi_2O_3 has lead to a good deal of research interest in the stabilization of this phase through solid solution formation [1–6], as well as the development of new families of bismuth oxide-based solid electrolytes. δ-Bi_2O_3 has a defect fluorite structure [7–11], with a high intrinsic vacancy concentration on the anion sublattice (a quarter of the available oxide ion sites are vacant). Combined with the high polarizability of the Bi atom

I. Abrahams (✉) · S. C. M. Chan
Centre for Materials Research,
School of Biological and Chemical Sciences,
Queen Mary,
University of London,
Mile End Road,
London E1 4NS, UK
e-mail: I.Abrahams@qmul.ac.uk

F. Krok · W. Wrobel · A. Kozanecka-Szmigiel ·
A. Luma · J. R. Dygas
Faculty of Physics, Warsaw University of Technology,
ul. Koszykowa 75,
00-662 Warsaw, Poland
e-mail: fkrok@mech.pw.edu.pl

with its $6s^2$ lone pair of electrons, conductivity values in the region of 1 S cm^{-1} at temperatures above 730°C are achieved [12].

While much research on stabilization of δ-Bi_2O_3 has involved substitution of Bi^{3+} by rare earth cations, it has been shown that many other cations are also suitable substituents for Bi^{3+} giving rise to *fcc* and rhombohedral fluorite phases (these are reviewed in references [2] and [4]). Amongst these, Nb^{5+} is found to substitute over a wide composition range, resulting in phases of general composition $Bi_{2-x}Nb_xO_{3+x}$ [13–15], which show superlattice ordering of the *fcc* fluorite cell. Zhou et al. [13] classified the superlattice ordering in this system as belonging to four basic types depending on composition. Of particular interest is the composition Bi_3NbO_7, the structure of which has recently been shown to exhibit superlattice ordering [16].

The superlattice ordering as well as the lower vacancy concentration in Bi_3NbO_7 compared to Bi_2O_3 result in a lower conductivity for Bi_3NbO_7. However, we have shown, that substitution of Nb^{5+} by subvalent cations such as Zr^{4+} [17] and Y^{3+} [18, 19] not only results in an increase in vacancy concentration, but also a compositionally dependent removal of superlattice ordering. These features, combined with a lattice expansion, yield a conductivity increase with respect to the parent Bi_3NbO_7. One of the most important influences on ionic mobility is the polarizibility of the immobile sublattice. It has been shown that ionic conductivity in stabilized Bi_2O_3 based electrolytes can be increased by additional substitution with highly polarizable dopants such as tungsten [20]. We have shown through computer simulation techniques that W^{6+} has a very favorable solution energy for Nb^{5+} substitution in Bi_3NbO_7 [21] and, therefore, solid solution formation is predicted.

The two most important contributions to ionic conductivity are charge carrier concentration and ionic mobility. In the present study, we examine substitution of Nb^{5+} by W^{6+} in Bi_3NbO_7. This substitution reduces the overall charge carrier (oxide ion vacancy) concentration. The influence of the tungsten dopant on mobility is more complex. Doping

with tungsten has the potential to increase mobility due to an overall increase in polarizability of the immobile sublattice. However, supervalent substitution such as that in the present system can lead to an increased dopant–vacancy interaction and, hence, lower mobility. In this study, we present a detailed investigation of defect structure and electrical conductivity in $Bi_3Nb_{0.8}W_{0.2}O_{7.1}$ using a combination of X-ray and neutron diffraction and AC impedance spectroscopy.

Experimental

Preparations

Samples of $Bi_3Nb_{1-x}Y_xO_{7-x}$ ($0.00 \leq x \leq 1.00$) were prepared using appropriate amounts of Bi_2O_3 (Aldrich, 99.9%), WO_3 (Aldrich, 99.99%), and Nb_2O_5 (Aldrich, 99.9%). Starting mixtures were ground in ethanol using a planetary ball mill. The dried mixtures were heated initially at 740°C for 24 h, then cooled, reground, and pelletized. Pellets were pressed isostatically at a pressure of 400 MPa, then sintered at 800°C for 10 h. Samples were slowly cooled in air to room temperature over a period of approximately 12 h.

Electrical measurements

Electrical parameters were determined by AC impedance spectroscopy up to *ca* 760°C using a fully automated Solartron 1255/1286 system in the frequency range 1 to 5×10^5 Hz. Samples for impedance measurements were prepared as rectangular blocks (*ca* $6 \times 3 \times 3$ mm^3) cut from slow-cooled sintered pellets using a diamond saw. Platinum electrodes were sputtered by cathodic discharge. Impedance spectra were carried out over two cycles of heating and cooling and collected at programmed temperatures after 15 min of temperature stabilization. Impedance at each frequency was measured repeatedly until consistency (2% tolerance in drift) was achieved or a maximum number of 25 repeats had been reached.

Crystallography

X-ray powder diffraction data were collected on an automated Philips PW1050/30 diffractometer using Ni-filtered CuKα radiation (λ=1.5418 Å) Data were collected in flat plate $\theta/2\theta$ geometry in steps of 0.02°, with a scan time of 2 s per step over the range 5 to 120° 2θ, with a scan time of 7 s per step. Calibration was carried out with an external Si standard.

Powder neutron diffraction data were collected on the Polaris diffractometer at the ISIS facility, Rutherford Appleton Laboratory. Data were collected on backscattering and low angle detectors over the respective time of flight ranges 1.0 to 20 and 0.5 to 20 ms. The samples were contained in cylindrical 11 mm vanadium cans located in front of the backscattering detectors. All data were collected at room temperature.

Structure refinement was carried out by combined Rietveld whole profile fitting of X-ray and neutron data sets using the program GSAS [22]. A cubic subcell model in space group *Fm*-3*m* was used for refinement; Bi, W, and Nb were located on the ideal 4*a* site 0,0,0 with oxide ions distributed over three sites: 8*c* at 0.25, 0.25, 0.25; 32*f* at approximately 0.3, 0.3, 0.3, and 48*i* at around 0.5, 0.2, 0.2 [10]. Crystal and refinement parameters are summarized in Table 1. The fitted diffraction profiles are shown in Fig. 1.

Results and discussion

Structure of $Bi_3Nb_{0.8}W_{0.2}O_{7.1}$

The X-ray diffraction profile for $Bi_3Nb_{0.8}W_{0.2}O_{7.1}$ does not show evidence of superlattice ordering and all peaks can be indexed on a cubic cell with *a*=5.47 Å (Fig. 1). In contrast, the neutron diffraction profiles show weak reflections clearly evident at around 5.02 Å and a cluster of peaks between 1.97 and 2.7 Å (Fig. 1b,c). These peaks are not indexable on the cubic cell, nor can they be attributed to starting materials or known phases within the system. The absence of these peaks in the X-ray pattern suggests that they are due to ordering over the oxide sublattice.

The structure of $Bi_3Nb_{0.8}W_{0.2}O_{7.1}$ was modelled using the cubic subcell and the refined structural parameters are shown in Table 2, with the derived contact distances in Table 3. The results show that the oxide ions are predominantly located in the 32*f* site, with no appreciable occupation of the ideal fluorite 8*c* site. This is in contrast to the situation in δ-Bi_2O_3 [7–11], but is consistent with the

Table 1 Crystal and refinement parameters for $Bi_3Nb_{0.8}W_{0.2}O_{7.1}$

Chemical formula	$Bi_3Nb_{0.8}W_{0.2}O_{7.1}$
Formula weight	851.63
Crystal system	Cubic
Space group	*Fm*-3*m*
Unit cell dimension	*a*=5.4676(4) Å
Volume	163.45(4) Å^3
Z	1
Density (calculated)	8.655 mg m^{-3}
Sample description	Yellow powder
R-factors[a]	
(a) X-ray	R_p=0.0973, R_{wp}=0.1253
	R_{ex}=0.0077, R_F2=0.1025
(b) Neutron backscattering	R_p=0.1003, R_{wp}=0.0541
	R_{ex}=0.0277, R_F2=0.2914
(c) Neutron low angle	R_p=0.0910, R_{wp}=0.1190
	R_{ex}=0.0919, R_F2=0.2691
Total number of variables	82
Number of profile points used	5,399 (X-ray)
	4,122 (neutron backscattering)
	4,332 (neutron low angle)

[a]For definition of *R*-factors see reference [22]

Fig. 1 Fitted diffraction profiles for $Bi_3Nb_{0.8}W_{0.2}O_{7.1}$ showing observed (*points*), calculated (*solid line*), and difference (*lower*) profiles, with reflection positions indicated by markers. **a** X-ray, **b** neutron back scattering, and **c** neutron low angle data are shown
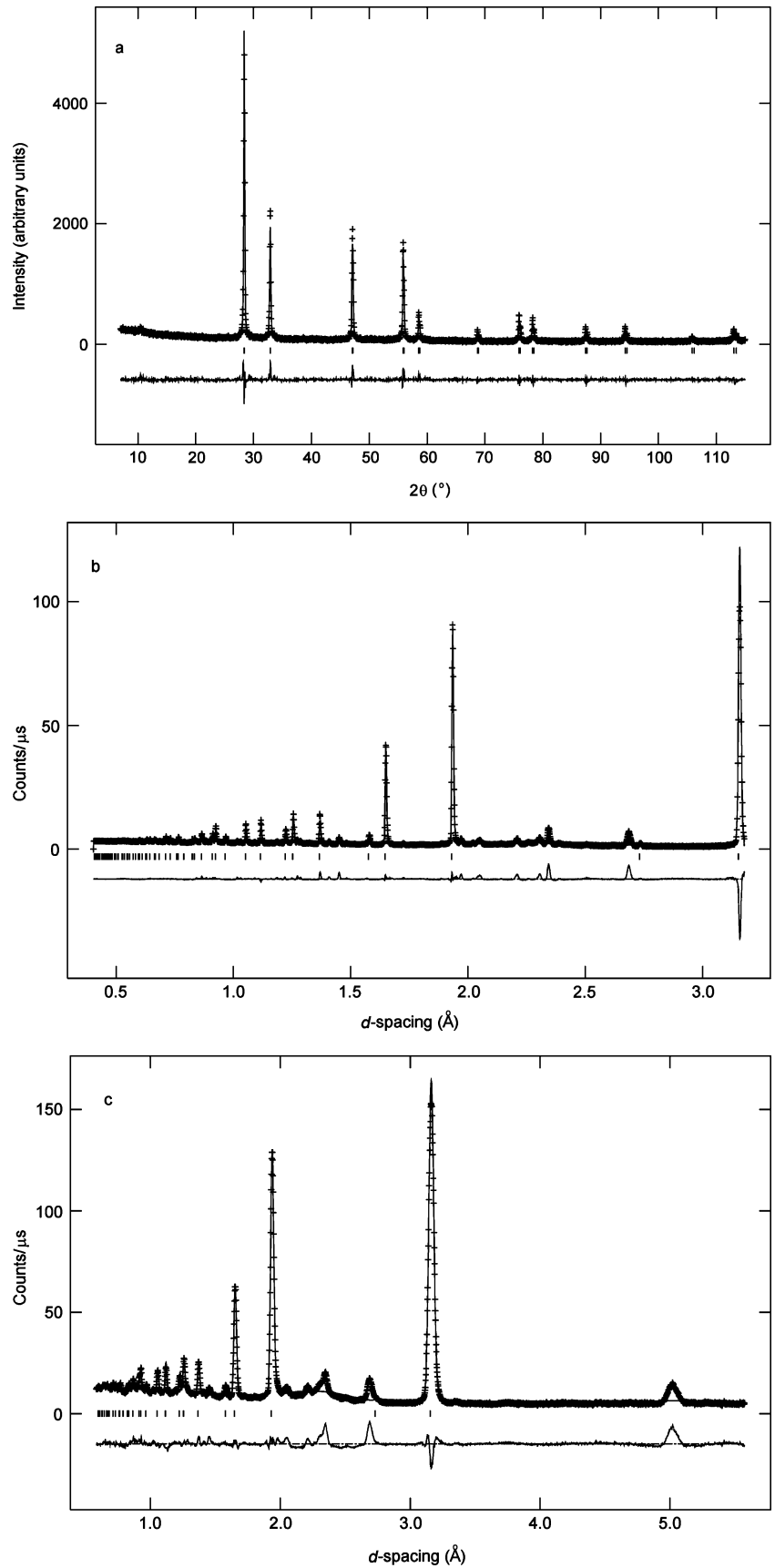
Table 2 Refined structural parameters for $Bi_3Nb_{0.8}W_{0.2}O_{7.1}$

Atom	Wyc.	x	y	z	Occ.	U_{iso} (Å^2)
Bi	4a	0.0(-)	0.0(-)	0.0(-)	0.75(-)	0.0194(1)
W	4a	0.0(-)	0.0(-)	0.0(-)	0.05(-)	0.0194(1)
Nb	4a	0.0(-)	0.0(-)	0.0(-)	0.20(-)	0.0194(1)
O(1)	32f	0.2843(6)	0.2843(6)	0.2843(6)	0.194(1)	0.087(2)
O(2)	48i	0.5(-)	0.248(11)	0.248(11)	0.019(1)	0.087(2)

system $Bi_3Nb_{1-x}Y_xO_{7-x}$ at similar levels of substitution [19]. There is also evidence of occupation of the 48i site by oxide ions as seen in other studies of doped bismuth oxide based fluorite structures (see for example reference [23]).

The 32f site, O(1), is close to the ideal fluorite 8c site (at 1/4, 1/4, 1/4). However, if ions were located in the ideal 8c site, they would coordinate four cations in a tetrahedral geometry, ions in the O(1) site coordinate only three cations, at a distance of 2.280 Å, resulting in a trigonal pyramidal geometry around O(1), with a fourth non-bonding contact to Bi of 2.692 Å. Oxide ions located in the 48i, O(2), site coordinate two cations in a linear geometry. This means that each O(1) atom is shared between three cations, while O(2) is shared between two cations.

Diffraction techniques, such as those used in the present study, yield an average picture of the structure. However, the crystal chemistry and preferred coordination geometries for the cations used in this study are well known. Taking the preferred coordination geometries into account, as well as partial site occupancies and short intersite contact distances, which preclude simultaneous occupation of sites, it is possible to derive cation coordination environments from the average picture generated from the structure refinement. A range of possible cation environments derived from the structure of $Bi_3Nb_{0.8}W_{0.2}O_{7.1}$ is illustrated in Fig. 2.

From the data in Table 2, the ratios of oxide ions in the two oxide sites to Bi^{3+}, Nb^{5+}, and W^{6+} cations can be calculated and it becomes evident that the O(2) to (Nb/W) ratio is close to 1. It is known that in the structure of δ-Bi_2O_3, there is no observed occupation of the 48i site [7–11]. It is therefore reasonable to suppose that O(2) might be exclusively associated with coordination to niobium and tungsten. Furthermore, if O(2) is exclusively associated with Nb^{5+} and W^{6+}, then the fact that O(2) coordinates two cations suggests clustering of these cations within the lattice. The approximate ratio of 1:1 for O(2) to (Nb/W) means that each Nb/W cation is coordinated to two shared O(2) atoms.

Before describing the defect structure in $Bi_3Nb_{0.8}W_{0.2}O_{7.1}$, it is helpful to start with a description of the situation in δ-Bi_2O_3. In crystalline oxides, Bi preferentially adopts a square pyramidal geometry as a result of the stereochem-

ical activity of the non-bonding $6s^2$ lone pair of electrons. In δ-Bi_2O_3, the Bi to O ratio is 1:1.5. Several studies on δ-Bi_2O_3 have shown occupation of combinations of the 8c and 32f sites [10, 11]. Depending on the relative occupancies of these sites, the average coordination number for Bi in δ-Bi_2O_3 ranges from 4.5 (for exclusive occupation of the 32f sites [9]) to 6 (for exclusive occupation of the 8c sites [7]). The neutron diffraction studies of Battle et al. [10] suggest simultaneous occupation of these sites resulting in an average coordination number of 5.36. More recently, the neutron diffraction study by Yashima and Ishimura [11] confirms simultaneous
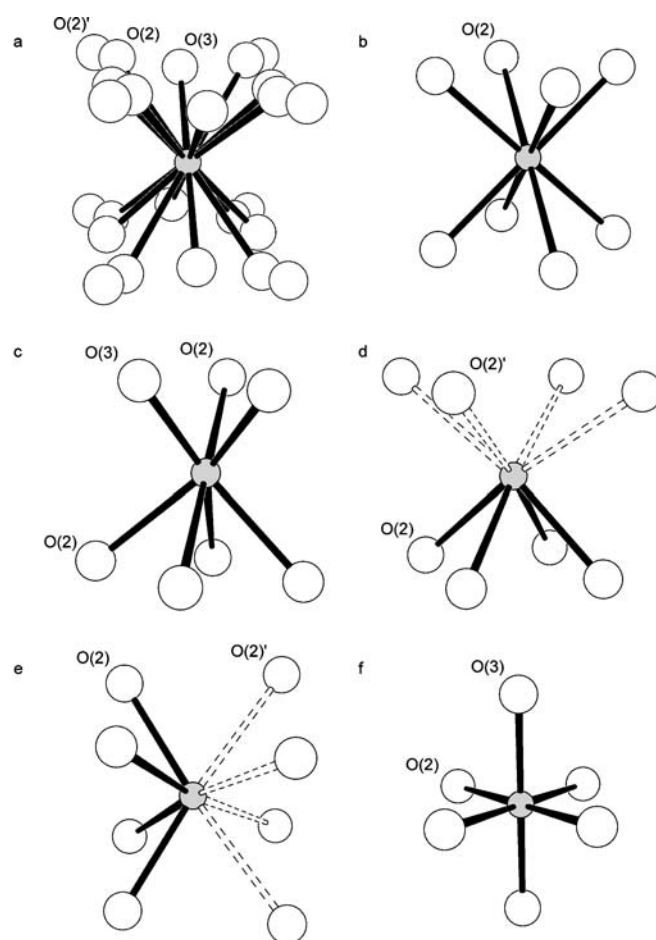
Fig. 2 Possible cation coordination geometries in $Bi_3Nb_{0.8}W_{0.2}O_{7.1}$, showing **a** all oxide ion sites, **b** eight coordination, **c** seven coordinate, **d** four-pyramidal coordination configuration 1 **e** four pyramidal configuration 2, and **f** distorted octahedral coordination. Cations (*shaded spheres*) and oxide ions (*large spheres*) are shown

Table 3 Significant contact distances (Å) in $Bi_3Nb_{0.8}W_{0.2}O_{7.1}$

Bi/Nb/W-O(1)	2.280(1)×8
Bi/Nb/W-O(1)′	2.692(6)×8
Bi/Nb/W-O(2)	1.933(1)×8

occupation of 8*c* and 32*f* sites, but with a lower average coordination number of 5.02.

In the present study, there appears to be no appreciable occupation of the 8*c* sites. This suggests that the average coordination number of Bi must be lower than six. If it is assumed that Bi in $Bi_3Nb_{0.8}W_{0.2}O_{7.1}$ is exclusively four coordinate, bonding to O(1), then it is possible to calculate the amount of oxide ions required to fulfill this coordination requirement and, hence, deduce from the remaining oxide ions the coordination number of the Nb^{5+}/W^{6+} cations. Four O(1) oxide ions per cell would be required for coordination to bismuth leaving 2.208 O(1) and 0.912 O(2) per cell for coordination to Nb^{5+} and W^{6+}. Because O(1) is shared between three cations and O(2) between two, this gives an average coordination number for Nb^{5+}/W^{6+} of 8.448 (3×2.208+0.912×2). Clearly this value is too high, which indicates that the average coordination number for Bi must be higher.

The crystal chemistry of niobium and tungsten oxides is dominated by six coordinate geometry for the cations. If it is assumed that this is also the case in the present study, then this would require 1 O(2) and 1.33 O(1) atoms per cell. This compares favorably with the observed value for O(2) of 0.912 per cell. This would leave 4.77 O(1) for coordination to Bi per cell, i.e., an average coordination number of 4.77 (4.77×1/3×3) for Bi. This value lies well within the range calculated for Bi in δ-Bi_2O_3. The assumption of six-coordinate geometry for Nb^{5+} is supported by the recent structure determination of Bi_3NbO_7, which indeed shows Nb^{5+} in six-coordinate geometry [16].

An average coordination number of 4.77 for bismuth can derived through a combination of four-pyramidal (Fig. 2d,e) and eight coordinate (Fig. 2b) geometries, with 80.75% of the Bi in the former coordination geometry and 19.25% in the latter. Similar calculations can be performed assuming lower coordination geometries for Bi.

Electrical conductivity of $Bi_3Nb_{0.8}W_{0.2}O_{7.1}$

Separation of grain boundary and intragrain conductivity in impedance spectra for $Bi_3Nb_{0.8}W_{0.2}O_{7.1}$ was only possible at very low temperatures and, therefore, only total conductivities are discussed in this study. The Arrhenius plot of total conductivity for $Bi_3Nb_{0.8}W_{0.2}O_{7.1}$ is shown in Fig. 3. On heating of a single linear region is observed throughout the temperature range studied. In contrast, on cooling the heating plot is reproduced down to around 600°C, whereupon a subtle deviation from linearity is observed leading to a second linear region of lower activation energy. This type of behavior has been correlated with temperature dependent changes in the defect structure in the analogous system $Bi_3Nb_{1-x}Y_xO_{7-x}$, involving changes in the relative occupancies of 8*c*, 32*f*, and 48*i* oxide-ion sites [19]. The similarity of the defect structure in $Bi_3Nb_{0.8}W_{0.2}O_{7.1}$ to that in $Bi_3Nb_{1-x}Y_xO_{7-x}$ and the observation of similar temperature-dependent behavior of conductivity in both systems suggests that the behavior

observed in the present study may also be explained by temperature dependent changes in the defect structure.

The values for total conductivity at 300 and 600°C (σ_{300} and σ_{600}) of 3.07×10^{-7} and 2.76×10^{-4} S cm^{-1}, respectively, are lower than the corresponding values in the parent material Bi_3NbO_7 (σ_{300}=2.6×10^{-6} S cm^{-1} and σ_{600}=9.36×10^{-4} S cm^{-1} [17]). This decrease in conductivity can be explained by the reduction in oxide ion vacancy concentration with respect to Bi_3NbO_7. Furthermore, if Nb^{5+} and W^{6+} do indeed favor six coordinate geometry in $Bi_3Nb_{0.8}W_{0.2}O_{7.1}$, as indicated by our structural study, this implies the trapping of an average of one oxide ion vacancy in the coordination sphere of these cations, therefore, further reducing the total number of effective charge carriers.

The activation energies for high and low temperature regions (ΔE_{HT} and ΔE_{LT}) of 1.23 and 1.03 eV, respectively, are higher than those seen in Bi_3NbO_7 (ΔE_{HT}=0.90 eV and ΔE_{LT}=0.90 eV [17]). In $Bi_3Nb_{0.8}W_{0.2}O_{7.1}$, the increase in activation energy with respect to that in Bi_3NbO_7 can be attributed to an increased dopant–vacancy interaction in the present system, due to the increased cation charge of W^{6+} compared to Nb^{5+}.

Conclusions

$Bi_3Nb_{0.8}W_{0.2}O_{7.1}$ exhibits a defect fluorite structure with evidence of superlattice ordering of the oxide ion sublattice. The vacancy concentration is lower than that in the parent Bi_3NbO_7 and this is reflected in a lower value of total conductivity. The higher cation charge of W^{6+} compared to Nb^{5+} results in stronger dopant–vacancy interactions leading to higher activation energy for conduction and reduced ionic mobility. Nb^{5+} and W^{6+} are believed to exhibit six-coordinate geometry in $Bi_3Nb_{0.8}W_{0.2}O_{7.1}$. This has the effect of reducing the effective number of charge
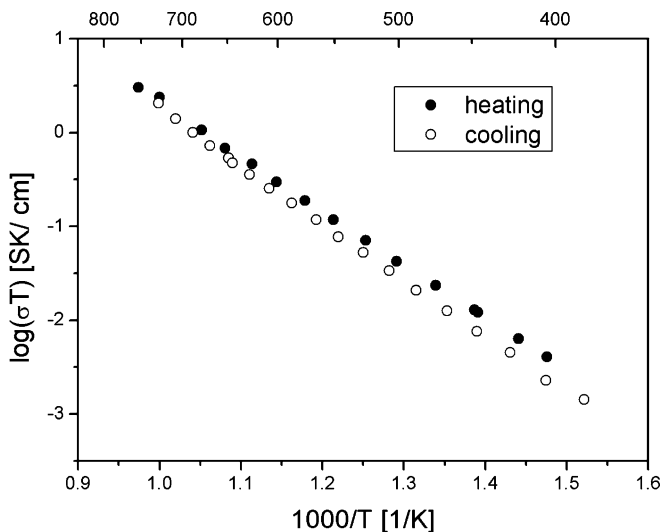

Fig. 3 Arrhenius plot of total electrical conductivity for $Bi_3Nb_{0.8}W_{0.2}O_{7.1}$. Heating (*filled circles*) and cooling (*open circles*) runs are shown

carriers through vacancy trapping in the coordination sphere of these cations. The average bismuth coordination number is 4.77, which can be modelled on a combination of square pyramidal and eight coordinate Bi. This value is similar to that derived from structural data for δ-Bi_2O_3.

References

1. Mairesse G (1993) In: Scrosati B, Magistris A, Mari CM, Mariotto G (eds) Fast ion transport in solids. Kluwer, Dordrecht, pp 271–290
2. Bovin JC, Mairesse G (1998) Chem Mater 10:2870
3. Shuk P, Wiemhöfer HD, Guth U, Göpel W, Greenblatt M (1996) Solid State Ionics 89:179
4. Sammes NM, Tompsett GA, Näfe H, Aldinger F (1999) J Eur Ceram Soc 19:1801
5. Azad AM, Larose S, Akbar SA (1994) J Mater Sci 29:4135
6. Goodenough JB, Manthiram A, Paranthaman M, Zhen YS (1992) Mater Sci Eng B12:357
7. Gattow G, Schroeder H (1962) Z Anorg Allg Chem 318:176
8. Hund F (1964) Z Anorg Allg Chem 333:248
9. Harwig HA (1978) Z Anorg Allg Chem 444:151
10. Battle PD, Catlow CRA, Drennan J, Murray AD (1983) J Phys C16:L561
11. Yashima M, Ishimura D (2003) Chem Phys Lett 378:395
12. Takahashi T, Iwahara H, Nagaj Y (1972) J Appl Electrochem 2:97
13. Zhou W, Jefferson DA, Thomas JM (1986) Proc R Soc Lond A 406:173
14. Ling CD, Withers RL, Schmid S, Thompson JG (1988) J Solid State Chem 137:42
15. Castro A, Aguado E, Rojo JM, Herrero P, Enjalbert R, Galy J (1988) Mater Res Bull 33:31
16. Ling CD, Johnson M (2004) J Solid State Chem 177:1838
17. Krok F, Abrahams I, Wrobel W, Chan SCM, Kozanecka A, Ossowski T (2004) Solid State Ionics 175:335
18. Kozanecka A, Krok F, Abrahams I, Wrobel W, Chan SCM, Dygas JR (2006) Mater Sci-Poland (in press)
19. Abrahams I, Kozanecka-Szmigiel A, Krok F, Wrobel W, Chan SCM, Dygas JR (2006) Solid State Ionics (in press)
20. Jiang N, Wachsman Ed, Jung S-H (2002) Solid State Ionics 150:347
21. Kozanecka-Szmigiel A, Krok F, Abrahams I, Islam MS (to be published)
22. Larson AC, Von Dreele RB (1987) Los Alamos National Laboratory Report, No. LAUR-86–748
23. Boyapati S, Wachman ED, Jiang N (2001) Solid State Ionics 140:149